



Pergamon

5*H*-8,9-Dimethoxy-5-(2-*N,N*-dimethylaminoethyl)dibenzo[*c,h*][1,6]naphthyridin-6-ones and Related Compounds as TOP1-Targeting Agents: Influence of Structure on the Ternary Cleavable Complex Formation

John E. Kerrigan,^{a,b,*} Daniel S. Pilch,^{a,b} Alexander L. Ruchelman,^c Nai Zhou,^a Angela Liu,^a Leroy Liu,^{a,b} and Edmond J. LaVoie^{b,c}

^aDepartment of Pharmacology, The University of Medicine and Dentistry of New Jersey, Robert Wood Johnson Medical School, Piscataway, NJ 08854, USA

^bThe Cancer Institute of New Jersey, New Brunswick, NJ 08901, USA

^cDepartment of Pharmaceutical Chemistry, School of Pharmacy, Rutgers University, Piscataway, NJ 08854-8020, USA

Received 30 May 2003; revised 23 July 2003; accepted 29 July 2003

Abstract—In this paper, we present our results from a docking study of the title compounds with the DNA/topoisomerase I complex based on the recently published X-ray crystal structure of the topotecan/DNA/topoisomerase I ternary cleavable complex (Staker, B.L., et al. *PNAS* **2002**, 99, 15387) using the Autodock program. Simple intermolecular docking energies (E_{dock}) correlate well with in vitro DNA cleavage data suggesting that the binding mode from the crystal structure is a reasonable binding mode for these compounds.

© 2003 Elsevier Ltd. All rights reserved.

Topoisomerase I is an important enzyme for cellular replication. The principal function of this enzyme is to relax supercoils in DNA during S-phase. The enzyme performs this function by making a nick or cut in the DNA followed by rotation about the complement phosphodiester bond to relieve the supercoil. The DNA is religated and the process continues. Drugs that target topoisomerase I (TOP1) are effective anticancer agents. Among these agents, the camptothecin family of compounds has been the most widely studied.¹ Of this broad and diverse family, Topotecan (Hycamtin[®]) and Irinotecan (CPT-11/Camptosar[®]) are the clinically relevant analogues. Unfortunately, this family of compounds suffers from hydrolytic instability in its δ -lactone ring system (the E ring in Fig. 1) and the clinically relevant analogues, topotecan and irinotecan, are substrates for efflux transporters leading to resistance.^{2–5} The ring-opened hydrolysis product binds to serum albumin further reducing the drug's efficacy.⁶

Topoisomerase-targeting agents bind to and stabilize the enzyme–DNA complex. A recent crystal structure published by Stewart, et al. of the topotecan/DNA/TOP1 ternary cleavable complex (1K4T.PDB) reveals a complex which is stabilized by intercalation of the drug between the +1 and –1 bases in the cleavage site.⁷ We were intrigued by the binding mode presented in this structure and decided to investigate this possible binding mode with a novel series of non-camptothecin topoisomerase I targeting agents.

Recent studies have demonstrated that compounds **1** and **2** (see Fig. 2) are highly active TOP1-targeting agents that exhibit potent cytotoxicity.^{8,9} Compounds **1**

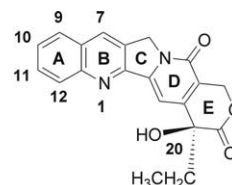


Figure 1. Camptothecin ring structure.

*Corresponding author. Tel.: +1-732-235-4473; fax: +1-732-235-5252; e-mail: kerrigje@umdnj.edu

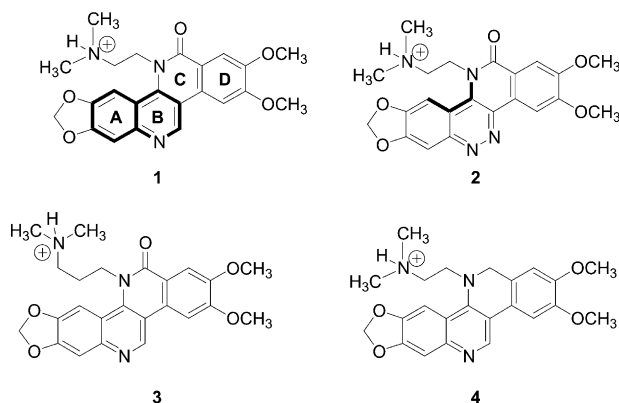


Figure 2. Methylenedioxy compounds **1–4**.

and **2** have a quinoline ring structure (outlined in bold bonds in compound **1** in Fig. 2) in common with the camptothecins (Fig. 1) as well as the same sensitivity to cross-resistance to mutations in topoisomerase I. In addition, these compounds have a dimethylammonium ion in the same relative proximity of the structure as does topotecan (topotecan has a (dimethylammonium)methyl group in the 9-position). Stewart's crystal structure indicates that the twist between the –1 thymine base and its adenine complement is $\sim 12^\circ$. The twist noted in the dihedral angles (see the bold bonds on compound **2** for the dihedral angle location in Fig. 2) between the A/B and C/D rings of our compounds (Figs. 2 and 3) is on the order of $14\text{--}17^\circ$ (except for compound **8** which is $\sim 26^\circ$). Using the published X-ray crystal structure of the topotecan/DNA/TOP1 complex (1K4T.PDB) mentioned earlier as a template, we performed a docking study of these and other analogues.

The individual compounds were built in MOE (Chemical Computing Group, Inc.) and refined using a systematic conformer search followed by geometry optimization of the lowest energy structure using the Merck Molecular Force Field (MMFF94).¹⁰ The individual compounds were pre-positioned based on the coordinates of the A and B rings (the quinoline ring unit) of topotecan from the X-ray structure. The side chains of the disordered amino acid residues of the macromolecule complex (1K4T.PDB) were rebuilt in

DeepView.¹¹ The water molecules, Hg atom, topotecan molecule, and polyethylene glycol molecule were all removed. The 5'-thioguanine was converted to a normal guanine residue. Polar hydrogen atoms were added to the protein–DNA complex and AMBER RESP charges loaded followed by energy minimization of the hydrogen atom positions only using the AMBER94 force field in MOE.¹² The small molecule compounds and the macromolecule were further processed using the AutoDock Tool Kit (ADT).¹³ Gasteiger–Marsili charges¹⁴ were loaded on the small molecules in ADT. Cornell parameters¹² were used for the phosphorous atoms in the DNA. All docking runs were performed using AutoDock v 3.0.5's Lamarckian Genetic Algorithm¹⁵ with grid dimensions of $90 \times 90 \times 46$ npts and a grid spacing of 0.200 Å. Autodock does not have solvation or fragmental volume parameters for the nucleic acid portion of the complex. Therefore, the simpler intermolecular energy function based on the Weiner force field¹⁶ in Autodock was used to score the docking results.

For this study we opted to compare a group of methylenedioxy analogues (compounds **1–4** in Fig. 2 with a methylenedioxy ring fused to the A ring) against a group of less potent analogues with a nitro substituent in the A ring (compounds **5–8** in Fig. 3). In our analysis of the docking results, we screened out all other orientations save the topotecan binding orientation. The results are listed in Table 1. The topoisomerase I-mediated DNA cleavage values are reported as REC, Relative Effective Concentration, that is, concentrations relative to topotecan, whose value is arbitrarily assumed as 1.0, that are able to produce the same cleavage on the plasmid DNA in the presence of human topoisomerase I. The overall plot of the data (not shown) had a low correlation ($R^2=0.75$); however, within the compound subgroups (methylenedioxy and nitro) we observe a very good linear correlation between $\ln(\text{REC})$ (an in vitro measure of DNA cleavage) and E_{dock} (see Figs. 4 and 5).

The interactions between a selection of the compounds in this study and the DNA/TOP1 complex are given in Figure 6 with corresponding stereoviews in Figure 7. We selected a strong compound (**1**), a midrange compound

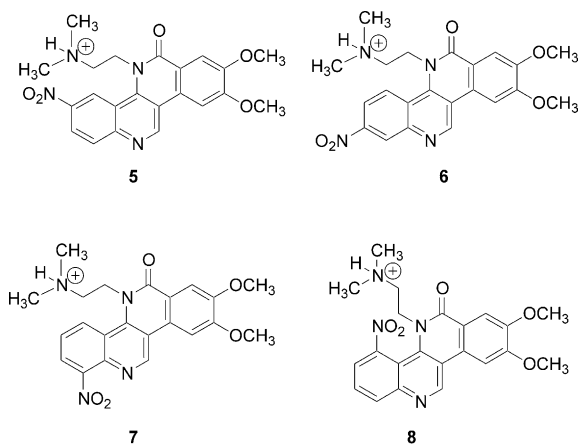


Figure 3. Nitro compounds **5–8**.

Table 1. Autodock energies and TOP1 cleavage data

Compd	E_{dock} (kcal/mol) ^a	RMSD (Å) ^b	TOP1 cleavage data (REC) ^c
1	–20.3	2.3	0.5
2	–21.0	3.3	0.3
3	–20.0	2.3	1
4	–19.9	2.3	0.8
5	–13.2	2.3	2
6	–12.2	2.3	6
7	–12.0	2.0	9
8	–10.0	2.3	300

^a $E_{\text{dock}} = E_{\text{vdw}} + E_{\text{elec}} + E_{\text{HB}} + E_{\text{int}}$ (where E_{int} is the internal energy of the ligand).

^bRMSD, root mean square deviation from initial position.

^cREC, effective concentration relative to topotecan (see text for details).

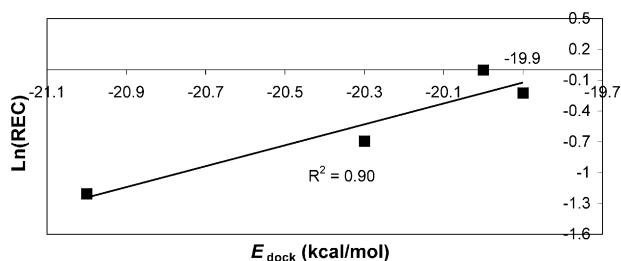


Figure 4. Plot of compounds 1–4.

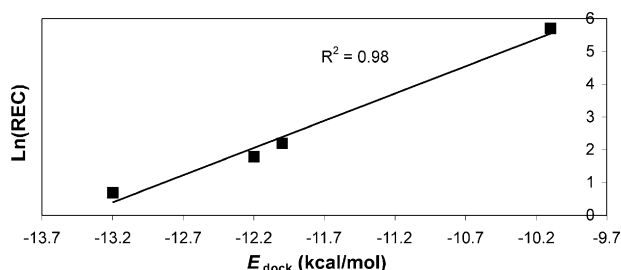


Figure 5. Plot of compounds 5–8.

(5) and the worst compound (8) in terms of DNA cleavage ability for illustration. All of the interactions listed in panels A and B in Figure 6 are hydrogen bonds. We used the criteria (angle and length) described by Chapman¹⁷ for classification of hydrogen bonds in our models. The interaction depicted in panel C of Figure 6 is a weak electrostatic, but too distant to be classified a hydrogen bond. Compounds 1 and 5 have the similar interactions with the complex. A hydrogen bond between the guanidinium ion hydrogen atom of ARG364 and the quinoline ring nitrogen atom of the B ring of compound 1 is observed. A hydrogen bond between the dimethylammonium ion hydrogen atom and the carbonyl oxygen atom of the +1 guanine base with hydrogen bonds between the amide hydrogen of ASN722 and the alcohol hydrogen of THR718 with the methoxy oxygen atoms of the D ring. These hydrogen-bonding interactions are also noted for compound 5. The principal difference between compounds 1 and 5 is in the A ring. The methylenedioxy ring fused to the A ring in compound 1 is better tolerated because it is more planar and does not have a steric clash with the DNA sugar backbone. However, the nitro group on the A ring in compound 5 has a moderate steric interaction with the DNA sugar backbone. In addition, the nitro group pulls electron density away from the quinoline nitrogen atom in the B ring making it a poorer hydrogen-bonding partner with ARG364. In compound 6 the position of the nitro group gives a slightly worse steric clash with the sugar backbone in comparison with compound 5. The nitro group in compound 7 is perpendicular to the plane of the A/B rings due to its interaction with the lone pair of the nitrogen atom in the B ring leading to an unfavorable steric interaction with the adenine base. We see in panel C of Figure 6 that compound 8 has lost all stabilizing hydrogen-bonding interactions. The severe twist in the ring system of compound 8, due to the steric clash between the nitro group on the A ring

and the (*N,N*-dimethylammonium)ethyl substituent, prevents compound 8 from fully intercalating between the +1 and –1 bases and their complements. This partial intercalation in compound 8 is manifested by a steric clash between its C and D rings with the –1 thymine base. Compounds 1 through 4 have more complex differences in their respective structures, yet there is good correlation in this group. The additional nitrogen atom in the B ring of compound 2 may make a better hydrogen-bonding partner with ARG364. Compound 3 has added flexibility in its (*N,N*-dimethylammonium)-propyl side chain, which is free to flex around in the wide open major groove pocket. In fact, the flexibility in

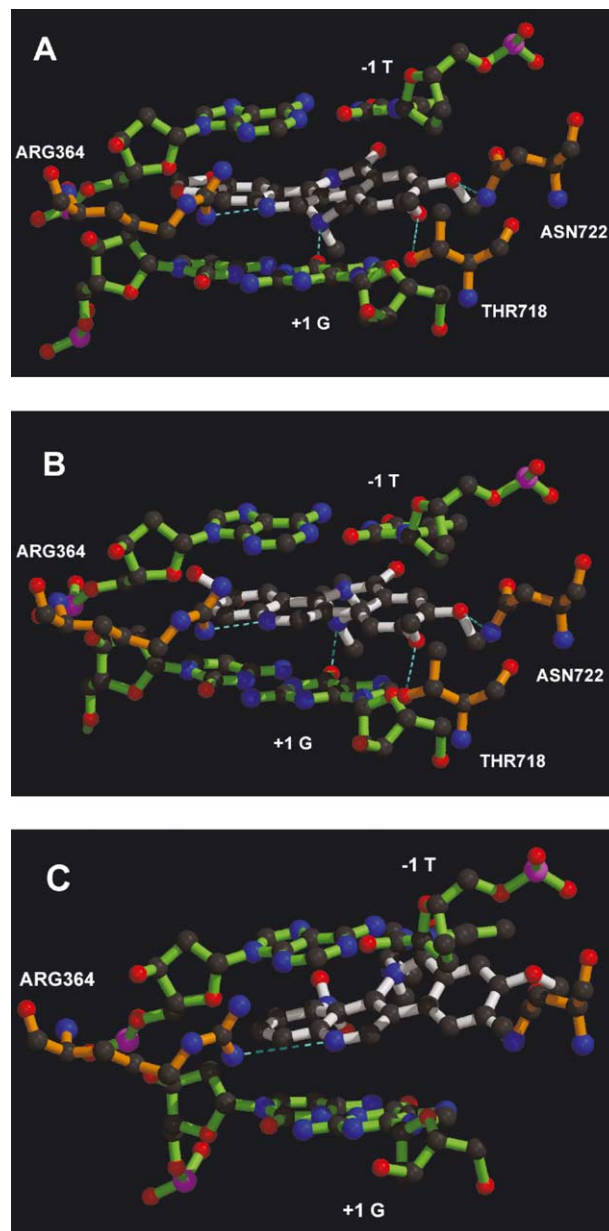


Figure 6. Comparison of low energy dock structure interactions. The hydrogen atoms have been omitted for clarity. The cyan hashed line indicates either a hydrogen bonding or electrostatic interaction. The different molecule types in the panels have their bonds color-coded according to the following Scheme: DNA—green; amino acids—orange; drug or ligand—white. Panel A: compound 1, Panel B: compound 5, Panel C: compound 8.

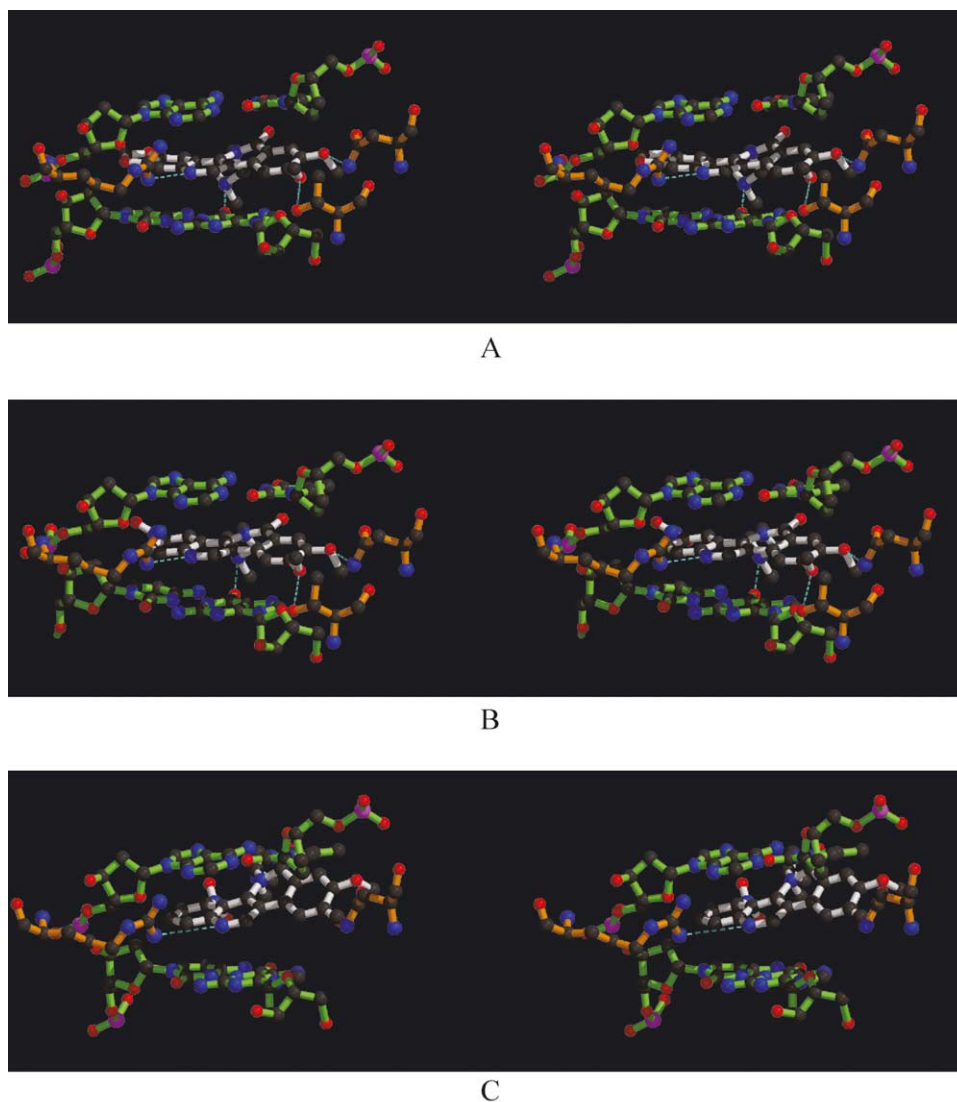


Figure 7. Stereoviews of the same panels described in Figure 6.

this side chain in compound **3** may be a cause for loss in correlation with experimental data. The removal of the carbonyl group in compound **4** gives more flexibility to the (*N,N*-dimethylammonium)ethyl side chain in this compound while keeping the relative twist between the rings. The illustrations in Figures 6 and 7 were prepared using Molscript¹⁸ and Raster 3-D.¹⁹

In conclusion, the dihedral twist in the ring system of our compounds is consistent with the concept of these drugs acting as base pair mimics as hypothesized for topotecan by Stewart et al. from their crystal structure.⁷ The docking results of these compounds using the fully intercalated binding mode of topotecan show good correlation with in vitro experimental DNA cleavage data and provide a reasonable explanation for the range in activity when one evaluates the models. Therefore, the binding mode derived from the crystal structure is a plausible model for the design of novel more efficacious

inhibitors of topoisomerase I based on the class of compound presented in this paper.

It has been demonstrated by crystallography that similar analogues of a drug may not bind in a similar fashion to complex targets possessing multiple binding pockets.²⁰ A previous modeling study of camptothecin analogues supported a binding orientation with the 'E'-ring pointed into the minor groove region.²¹ This orientation is perpendicular to the orientation found in the topotecan crystal structure. We must note that this perpendicular orientation was a second less predominant low energy orientation produced in the docking runs and indeed was lower in energy for a few of the analogues (most notably compound **8**). Due to the intricate nature of the DNA/TOP1 complex, these compounds may be capable of accessing multiple binding modes (i.e., their reaction kinetics may be biphasic). However, a rigorous experimental investigation of the

reaction kinetics will be needed to help support this hypothesis. Future investigation will focus on additional binding modes and the impact of solvent on this model.

Acknowledgements

This study was supported by Grant CA39662 (L.F.L.) and Grant CA077433 (L.F.L.) from the National Cancer Institute.

References and Notes

1. Ulukan, H.; Swaan, P. W. *Drugs* **2002**, *62*, 2039.
2. Chen, A. Y.; Yu, C.; Potmesil, M.; Wall, M. E.; Wani, M. C.; Liu, L. F. *Cancer Res.* **1991**, *51*, 6039.
3. Kawabata, S.; Oka, M.; Shiozawa, K.; Tsukamoto, K.; Nakatomi, K.; Soda, H.; Fukuda, M.; Ikegami, Y.; Sugahara, K.; Yamada, Y.; Kamihira, S.; Doyle, L. A.; Ross, D. D.; Kohno, S. *Biochem. Biophys. Res. Commun.* **2001**, *280*, 1216.
4. Saleem, A.; Edwards, T. K.; Rasheed, Z.; Rubin, E. H. *Ann. N.Y. Acad. Sci.* **2000**, *922*, 46.
5. Yang, C. H.; Schneider, E.; Kuo, M. L.; Volk, E. L.; Rochi, E.; Chen, Y. C. *Biochem. Pharmacol.* **2000**, *60*, 831.
6. Burke, T. G.; Mi, Z. *Anal. Biochem.* **1993**, *212*, 285.
7. Staker, B. L.; Hjerrild, K.; Feese, M. D.; Behnke, C. A.; Burgin, A. B.; Stewart, L. *PNAS* **2002**, *99*, 15387.
8. Ruchelman, A. L.; Singh, S. K.; Ray, A.; Wu, X.; Yang, J.-M.; Li, T.-K.; Liu, L. F.; LaVoie, E. J. *Bioorg. Med. Chem.* **2003**, *11*, 2061.
9. Ruchelman, A. L.; Singh, S. K.; Wu, X.; Ray, A.; Yang, J.-M.; Li, T.-K.; Liu, L. F.; LaVoie, E. J. *Bioorg. Med. Chem. Lett.* **2002**, *12*, 3333.
10. Halgren, T. J. *Comput. Chem.* **1996**, *17*, 490.
11. Guex, N.; Peitsch, M. C. *Electrophoresis* **1997**, *18*, 2714.
12. Cornell, W.; Cieplak, P.; Bayly, C.; Gould, I.; Merz, K.; Ferguson, D.; Spellmeyer, D.; Fox, T.; Caldwell, J.; Kollman, P. A. *J. Am. Chem. Soc.* **1995**, *117*, 5179.
13. Coon, S. I.; Sanner, M. F.; Olson, A. J. In *9th International Python Conference*, 2001; p. 1.
14. Gasteiger, J.; Marsili, M. *Tetrahedron* **1980**, *36*, 3219.
15. Morris, G. M.; Goodsell, D. S.; Halliday, R. S.; Huey, R.; Hart, W. E.; Belew, R. K.; Olson, A. J. *J. Comput. Chem.* **1998**, *19*, 1639.
16. Weiner, S. J.; Kollman, P. A.; Case, D. A.; Singh, U. C.; Ghio, C.; Alagona, G.; Profeta, S.; Weiner, P. *J. Am. Chem. Soc.* **1984**, *106*, 765.
17. Fabiola, F.; Bertram, R.; Korostelev, A.; Chapman, M. S. *Protein Sci.* **2002**, *11*, 1415.
18. Kraulis, P. J. *J. Appl. Cryst.* **1991**, *24*, 946.
19. Merritt, E. A.; Bacon, D. J. *Methods Enzymol.* **1997**, *277*, 505.
20. Mattos, C.; Rasmussen, B.; Ding, X.; Petsko, G.; Ringe, D. *Nat. Struct. Biol.* **1994**, *1*, 55.
21. Kerrigan, J. E.; Pilch, D. S. *Biochemistry* **2001**, *40*, 9792.